Science and Technology Indonesia
e-ISSN:2580-4391 *p*-ISSN:2580-4405
Vol. 10, No. 2, April 2025

Research Paper

Synthesis and Characterization of Composite Materials Based on Bacterial Cellulose and Fly Ash

Maya Yuliah[1], Teja Dwi Sutanto[2], Evi Maryanti[3], Eka Angasa[2], Irfan Gustian[3*]

[1]*Master Student Chemistry Program, Department of Chemistry, Faculty of Mathematics and Natural Sciences, University of Bengkulu, Bengkulu, 38371, Indonesia*
[2]*Master Chemistry Program, Department of Chemistry, Faculty of Mathematics and Natural Sciences, University of Bengkulu, Bengkulu, 38371, Indonesia*
[3]*Undergraduate Chemistry Program, Department of Chemistry, Faculty of Mathematics and Natural Sciences, University of Bengkulu, Bengkulu, 38371, Indonesia*
*__Corresponding author__: irfan.g@unib.ac.id

Abstract
The synthesis of composite materials based on bacterial cellulose with fly ash (FA) has been carried out based on the mass ratio between bacterial cellulose and fly ash, namely 0.005:4.995; 0.01:4.99; 0.015:4.985, and 0.02:4.98. Bacterial cellulose was obtained from the fermentation of coconut water and fly ash was treated after being obtained from the Steam Power Plant (PLTU) of Bengkulu Electric Power Plant Pulau Baai. The characterization of the composite material that had been formed was analyzed using Fourier Transform Infrared Spectroscopy (FTIR), X-ray diffraction (XRD), Raman Spectroscopy, and Scanning Electron Microscope (SEM), the results can be validated that the bacterial cellulose composite has been formed with fly ash. The FTIR results also support the XRD results that have been obtained, Raman spectroscopy shows a Raman shift at 1352 cm^{-1} as an indication of the bending of C−C−H, CH_2, and C−OH the highest conductivity was obtained in the variation of 0.02:4.98 which is 2.45×10^{-3} S/cm. The methanol permeability test obtained was higher along with the addition of fly ash to bacterial cellulose occurred in the composite material variation of 0.02:4.98, which is 3.66×10^{-9} mol/cm.s. The highest water absorption occurred in the composite material variation of 0.01:4.98 reaching 718% and the results of SEM micrographs with a magnification of 10000× produced a morphology in the form of fibers with fly ash components interwoven by bacterial cellulose fibers.

Keywords
Bacterial Cellulose, Fly Ash, Composite Materials, Methanol Permeability, Fibers

Received: 1 October 2024, Accepted: 24 February 2025
https://doi.org/10.26554/sti.2025.10.2.552-561

1. INTRODUCTION

Research that has tried to develop the utilization of natural biological sources is the manufacture of cellulose from coconut water known as bacterial cellulose, by utilizing the activity of *Acetobacter xylinum* bacteria (Iguchi et al., 2000; Thomas, 2008; Muhammad et al., 2014; Tahara et al., 1997). Other research related to its utilization as a material has been done by studying its performance as a dialysis membrane in a dilute solution system (Shibazaki et al., 1993). Then other reports have tried to study the physical and mechanical properties of thin layers of biocellulose (Moon et al., 2006; Nishi et al., 1990). It has been realized that natural biological materials that can be utilized for the manufacture of cellulose-based materials are quite available in our country, including bacterial cellulose made from coconut water known as nata de coco which can be made as a cellulose membrane material. Where the cellulose produced is chemically pure, free from lignin, has a high degree of crystallinity and degree of polymerization. Several researchers have studied its structure, physical properties and mechanical properties (Fontana et al., 1990; Henrik et al., 2006; Moon et al., 2015; Sulaeva et al., 2015).

Bacterial cellulose as a continuous phase for composite materials has been widely reported, ranging from modeling through computation (Rahmawati et al., 2018) to synthesis in the laboratory (Radiman and Rifathin, 2013; Aritonang et al., 2015; Aritonang et al., 2017). From previous studies it is known that phosphorylation of nata de coco as bacterial cellulose, obtained proton conductivity of 1.2×10^{-2} S/cm and a methanol permeability of 2.3×10^{-6} mol/cm.s (Radiman and Rifathin, 2013). These two parameters are important references in the development and utilization of bacterial cellulose as a continuous phase for composite materials, especially for Polymer Electrolyte Membrane Applications, moreover this reason is supported by previous studies related to the good physical and mechanical properties of bacterial cellulose. The properties and advantages of this bacterial cellulose as a biologically produced cellulose are shown from the resulting proton

conductivity of the order of minus 2.

The government's reliance on coal as its main source of energy for the production of power will undoubtedly lead to a number of environmental and health issues. One of them is caused by the existence of coal ash waste, often referred to as fly ash and bottom ash, which is classified as hazardous & toxic waste and is produced when coal is burned at PLTU. Government Regulation Number 101 of 2014 states that it comprises a hazardous & toxic waste component from a business's waste products, which needs to be processed and managed with extra care (Prayoga and Afla, 2023).

Indonesia is one of the largest coal producing countries in the world, where most of the coal is used as an energy source, namely as an energy source in Steam Power Plants. The construction of PLTU with a capacity of 35000 MW or 35 GW inside and outside Java Island is estimated to cause significant environmental damage if the remaining work produced is not used effectively, regarding environmental damage, it has been previously reported (Gopinathan et al., 2022). The waste disposed of from PLTU activities is in the form of coal ash in the form of fly ash and bottom ash.

The production of fly ash (FA) and bottom ash ranges from 6.15-8.5 million tons/year from coal use of 85 million tons/year in several countries in the world (Norhaiza et al., 2019). The fly ash produced contributes 80% and bottom ash contributes 20% of the remaining coal consumption. Steam Power Plant of Bengkulu Electric Power Plant Pulau Baai was established in February 2020 and is located in Teluk Sepang, Bengkulu City. The operational trial of the steam-powered power plant on October 7, 2021, which uses coal as fuel. In the process of combustion one million tons of coal per year at the Bengkulu PLTU, 200-250 tons of FA waste products are produced every day. Fly ash is a pozzolan containing alumina and silica that can be used as a substitute for cement with the addition of water (Joel, 2020). FA management is still limited to accumulation on unused land. Fly ash is a by-product of management produced from coal combustion. FA management is still limited to accumulation on unused land. Basically, fly ash has been used for a variety of products, including; the production of building materials such as cement, bricks, ceramics and paving, the production of concrete (Dheeresh et al., 2022). The FA is used to remove hazardous contaminants, organic and inorganic chemicals, and dyes from wastewater. Furthermore, research has revealed that FA has promising and beneficial potential applications in the construction industry, especially in the production of cement and concrete. FA has been added to cement in a reduced nano size form, thus providing good durability and minimizing the pore size of concrete to withstand adverse environments (Seham and Marei, 2021). Other previous studies, which examined the effect of adding fly ash (FA) as a partial cement substitute on the mechanical properties and characteristics of high-quality mortar, especially engineered cement mortar, have also been reported. The results of this study suggest that the use of FA waste as a substitute for cement provides an effective solution in managing industrial waste from FA, and Portland cement (Siregar et al., 2024).

Composites are alternative metal materials with several advantages such as lightweight, corrosion-resistant, and inexpensive materials and resistance to thermal conditions. Composites play an important role in the manufacturing industry. In this case, FA can be used as a carbon additive in carbon-based composites such as iron and steel. FA can also be used as a filler to improve the mechanical and thermal properties of composites (Kumar et al., 2018; Satapathy et al., 2012). Based on the abundance of FA and the research report above, it is necessary to process and research the FA waste produced into composite materials in order to reduce the amount of FA waste accumulation. In this report, a composite material based on bacterial cellulose and FA has been made. It is hoped that this composite material based on bacterial cellulose and fly ash can be tested for membranes in fuel cells.

2. EXPERIMENTAL SECTION

2.1 Materials

The materials used in this study were fly ash from the Steam Power Plant (PLTU) of Bengkulu Electric Power Plant Pulau Baai, coconut water obtained from traditional markets in Bengkulu city, distilled water, *Acetobacter xylinum*, ammonium sulfate (from Merck), glacial acetic acid (from Merck), sodium hydroxide (from Merck), and market granulated sugar.

2.2 Methods

2.2.1 Fly Ash Preparation

Fly ash preparation followed the modified Visa (2016) procedure. The fly ash obtained was washed using distilled water, then the sample was dried in direct sunlight using a container. After that, the sample was put into an oven at a temperature of 100°C for 3 hours until dry. The dried FA was ground with a mortar and pestle to form a finer powder. Then filtered through a 45 sieve. A total of 50 grams of fly ash powder was dissolved in 250 mL of 4 N HCl solution at a temperature of 70°C for 3 hours and stirred. NaOH solution was added to pH 7 at a temperature of 70°C until a gel was formed. The gel produced from the heating was centrifuged to separate the remaining solids and liquids, then reheated at a temperature of 70°C until dry and smoothed using a blender.

2.2.2 Preparation and Purification of Bacterial Cellulose

Preparation of bacterial cellulose was carried out by referring to the modified steps of Radiman and Yuliani (2008), by preparing three liters of coconut water that had previously been filtered and boiled. After boiling, the sample was added with 300 grams of fine sugar and 15 grams of ammonium sulfate, then transferred into a plastic container measuring 27 cm × 21 cm × 3.5 cm while hot and covered with newspaper. When the mixture is almost cold, open the cover and add 30 mL of glacial acetic acid. Close the plastic container again until the mixture is cold. After it has completely cooled, the cover is opened and 10% *Acetobacter xylinum* are added, then closed again to ferment for 10 days. The fermented bacterial cellulose was soaked

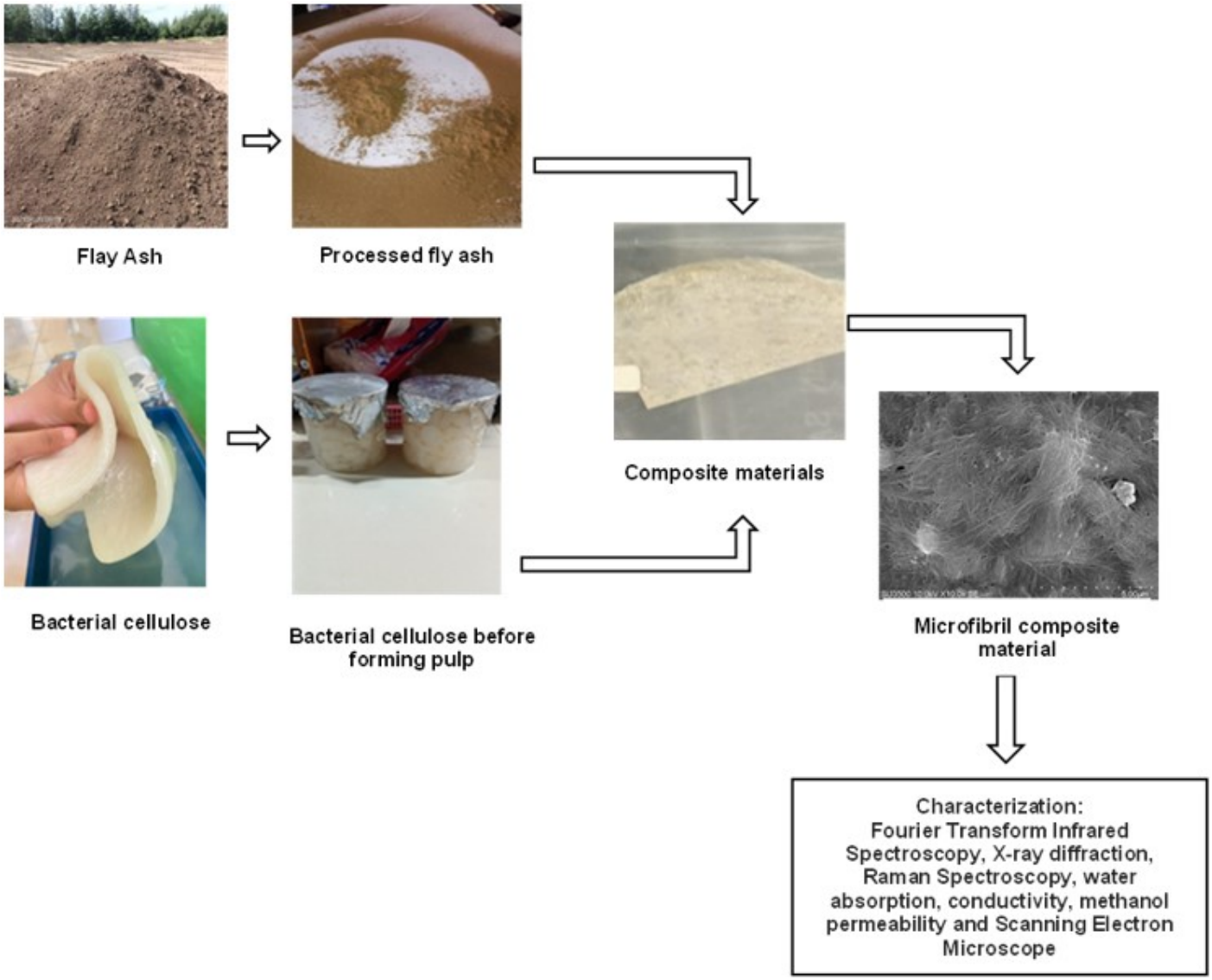

Figure 1. Scheme for Synthesis and Characterization of Composite Materials

in water for 24 hours using a beaker. Then soak it again in distilled water at a temperature of 80-90°C for 2 hours. Then soak it again in 2% NaOH at a temperature of 80-90°C for 2 hours. The last soaking used distilled water at a temperature of 80-90°C for 2 hours.

2.2.3 Synthesis of Composite Materials

The synthesis of composite materials refers to the method used by Gunday et al. (2021) which was modified. Bacterial cellulose was blended into a pulp and then filtered. The composite membrane was molded with a mass of 5 grams. Fly ash powder was then weighed with variations in content of the total mass used, then bacterial cellulose was added with a predetermined ratio. The mass ratio of fly ash powder to bacterial cellulose: respectively namely 0.005:4.995; 0.01:4.99; 0.015:4.985 and 0.02:4.98. The mixture was then stirred using a magnetic stirrer until homogeneous and then molded into a 5×5 cm diameter petri dish. After that, it was heated using a hot plate at a temperature of 30°C until a composite material in the form of a thin film was formed, released from the petri dish.

The composite material was then analyzed using Fourier Transform Infrared Spectroscopy (Bruker Alpha-P, Wismar, Germany in attenuated total reflectance (ATR) in range of 4000-400 cm^{-1}), X-ray diffraction (Rigaku DMAX2200, Japan) with Cu Ka (λ =1.5406 Å) radiation over the range 2θ between 0° and 70°, Raman Spectroscopy (Micro Confocal Hyperspectral 3D Imaging), Scanning Electron Microscope (JEOL JSM 6510 LA), The permeability of methanol was measured using a homemade test cell. The cell was filled with methanol. Methanol vapor in equilibrium with the liquid diffused along the concentration gradient through the membrane, which was clamped between the mouth of the beaker and its lid. The

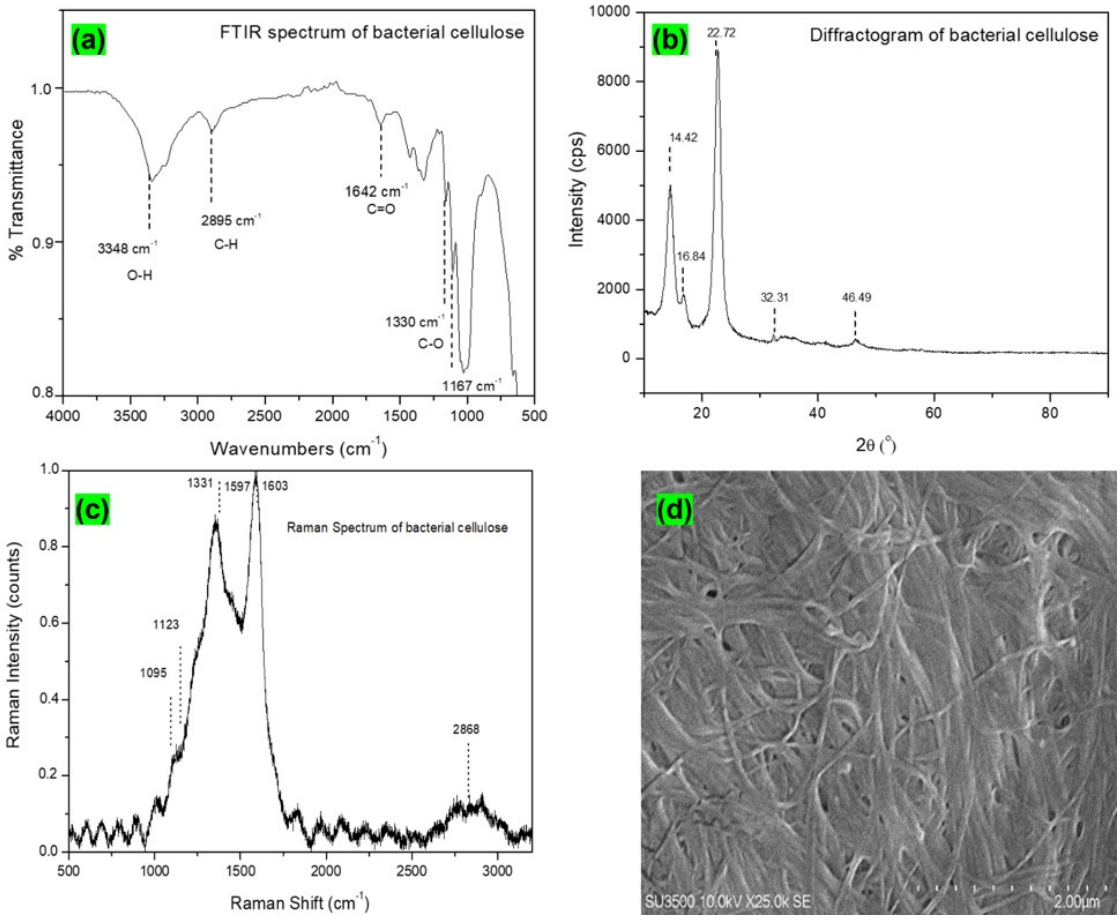

Figure 2. Characteristics of (a) FTIR Spectroscopy, (b) XRD, (c) Raman Spectroscopy and (d) Surface Micro-Profile of Bacterial Cellulose

weight loss was recorded as a function of time and the data were used for the calculation of permeability (Sen et al., 2008). Determination of water absorption capacity is determined gravimetrically and the conductivity of composite materials is measured using IM 3590 Chemical Impedancy Analyzer HIOKI. The research flow that has been carried out is shown in Figure 1.

3. RESULTS AND DISCUSSION

3.1 Fly Ash Preparation

The fly ash that has been obtained is then heated using an oven for 3 hours at a temperature of 100°C to remove the water content, then the dried FA is then filtered using a 45 mesh sieve. The obtained FA was mixed with 4 N HCl to remove unnecessary impurities. Then, NaOH was added to this mixture until a gel was formed. The gel formed was separated using centrifugation, so that the filtrate and residue were separated. Then, the centrifuged residue was taken and dried at a temperature of 70°C. With alkaline treatment, there will be an increase in Na in FA, then the following reaction occurs: NaOH + FA $Na_a(AlO_2)_b$ $(SiO_2)_c$ .NaOH.H_2O OH^- ions in basic solutions play a role in the dissolution stage of Si^{4+} and Al^{3+} from FA. The basic environment also forms active sites ≡SiO^- and ≡AlO (Visa, 2016).

3.2 Preparation and Purification of Bacterial Cellulose

The filtered coconut water is then boiled and added with granulated sugar and ammonium sulfate, then covered using newspaper. This is useful to avoid contamination from dust and other dirt. Then, after it has cooled slightly, glacial acetic acid is added to the coconut water. Then, when the coconut water mixture has cooled, *Acetobacter xylinum* bacteria are added and covered for 10 days. The use of coconut water in the production of bacterial cellulose is because coconut water can be converted into nata de coco by *Acetobacter xylinum* bacteria. The obtained bacterial cellulose was then soaked using NaOH for 2 hours. Soaking using NaOH solution can increase the purity of the cellulose produced, so that the bonds between cellulose chains become stronger due to the hydrogen bonds between chains, causing the bacterial cellulose structure to become thinner so that it becomes somewhat dense. The results of characterization of X-ray diffraction, Fourier Transform Infrared Spectroscopy, Raman Spectroscopy and surface micro

profiles of bacterial cellulose are shown in Figure 2.

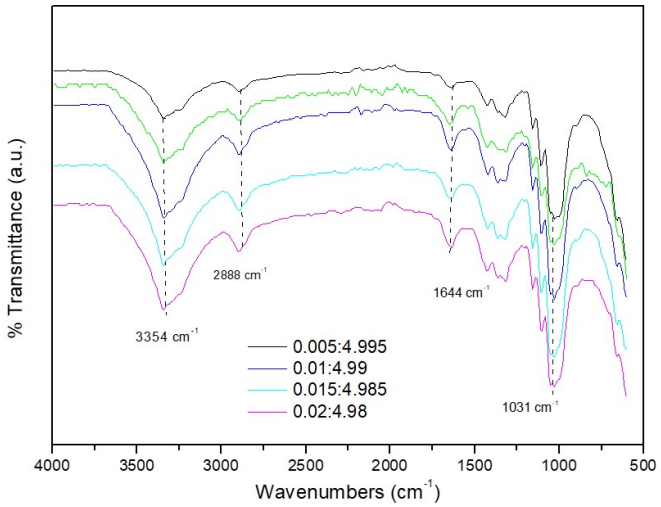

Figure 3. FTIR Spectra of Composite Materials

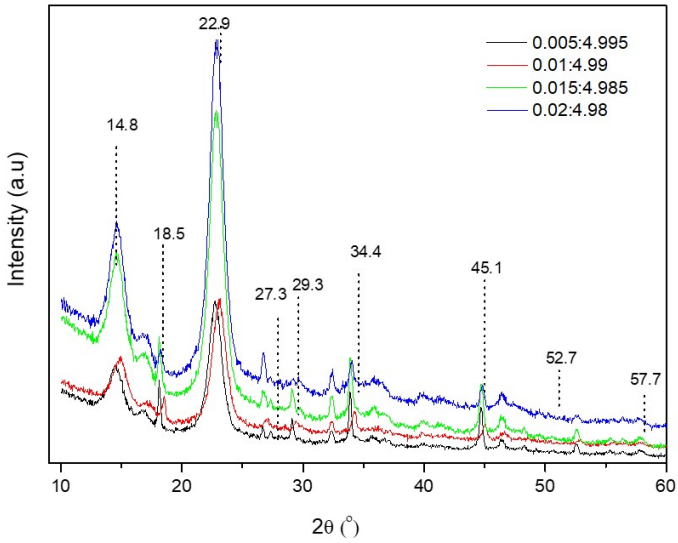

Figure 4. Diffractogram of Composite Materials

Characteristics of bacterial cellulose using FTIR in Figure 2(a) shows the spectrum of wave numbers at 3348 cm^{-1} which is the O−H functional group, 2895 cm^{-1} is the alkane group C−H, 1642 cm^{-1} and 1027 cm^{-1} are C=O groups, 1330 cm^{-1} and 1167 cm^{-1} are C−O groups. The results of determining these functional groups are based on previous studies (Radiman and Rifathin, 2013).The results of the characterization of bacterial cellulose using XRD in Figure 2(b) produce 2θ diffractograms at 14.42°, 16.64°, 22.72°, 32.31°, and 46.49°. The results of these 2θ indicate the diffractogram of bacterial cellulose, this characterization is also similar compared to previous studies shown in Figure 2 (Mutiara et al., 2022). From Raman characterization bacterial cellulose in Figure 2(c) shows Raman shift at 1095 cm^{-1} and 1123 cm^{-1} that corresponds to C−C and C−O stretching, and COC glycosidic asymmetric stretching, and area 1331 cm^{-1} was attributed to C−C−H, C−O−H, and O−C−H bending, 1597 cm^{-1} indicating C−O, 1603 cm^{-1} indicating ring stretching vibration, symmetrical vibration, 2868 cm^{-1} indicating stretching vibration of symmetric and asymmetric CH_2 (Refaat et al., 2023). An important

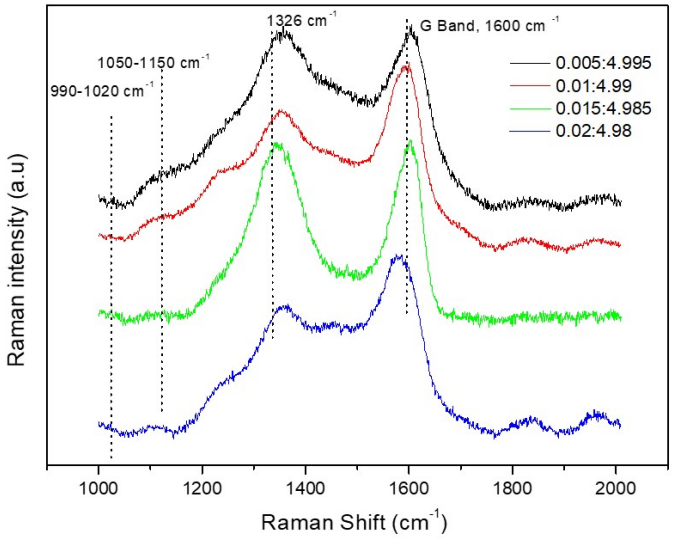

Figure 5. Raman Spectrum of Composite Materials

distinction between the Raman and IR spectra is the strength of the O−H stretching vibration in the 3200-3600 cm^{-1} region, which is quite weak in the Raman spectrum. This is due to the fact that there is a significant shift in the O−H vibration's dipole moment but a negligible change in polarizability. Because of the intricacy of the hydrogen bonding network in the crystal and the water molecules present in the amorphous area, the O−H stretching band is naturally broad. The C-H stretching vibration is responsible for the strong band that was detected in both Raman and IR spectra about 2900 cm^{-1}. The reasons behind the shoulder peaks located at the lower (2840-2880 cm^{-1}) and upper (2920-2970 cm^{-1}) energy sides of the C−H peak. The symmetric and asymmetric CH_2 stretching vibrations of the hydroxymethyl groups in cellulose are responsible for the energy sides of the C−H peak, respectively. The deformation vibration of the CH_2 group on C6, sometimes referred to as the scissoring mode, is observed in the 1450-1480 cm^{-1} range. CH_2 shaking and swaying, C−O−H bending, and C−C−H bending are the causes of the bands between 11200 and 1450 cm^{-1}. Glycosidic and alcohol C−O bond stretching modes, as well as backbone ring stretching, are seen in the range of 950 to 1150 cm^{-1}. Bending of the backbone bonds of C−C−C, C−O−C, O−C−C, and O-C-O contributes below 950 cm^{-1}, the result of similar compared to previous studies (Kim et al., 2013). Figure 2(d) shows the morphological image of bacterial cellulose using SEM. The micrograph results show the surface of bacterial cellulose in the form of long fibers. This result

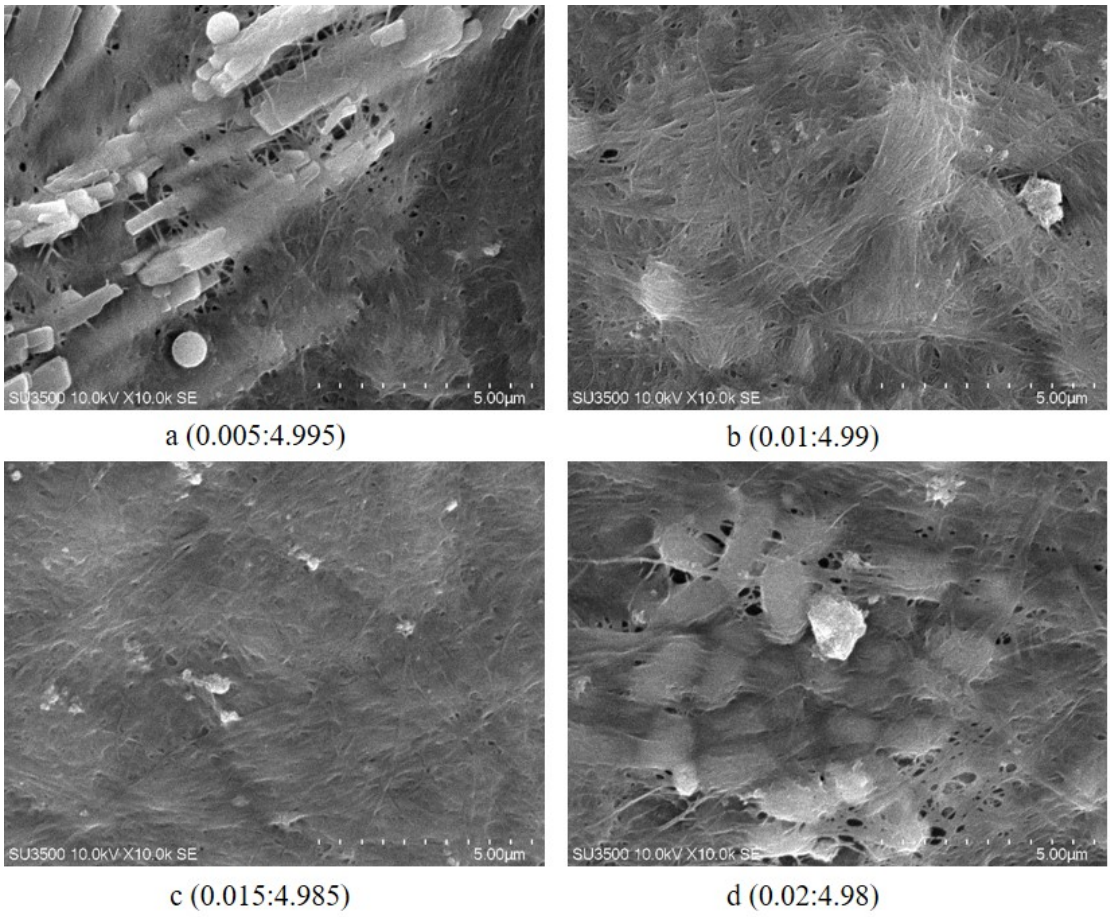

Figure 6. The Morphology of Composite Materials

is also supported by previous studies that produced bacterial cellulose in the form of fibers (Shao et al., 2016).

3.3 Synthesis and Characterization of Composite Materials

The results of the FTIR characterization of the composite material has been shown in the spectrum of Figure 3 which shows a typical wave number as a mixture of bacterial cellulose and fly ash, namely at 3354 cm^{-1} indicating the O−H stretching vibration, 2888 cm^{-1} is the C−H alkane functional group, 1644 cm^{-1} and 1031 cm^{-1} are the C−O functional groups. The wave number is the wave number of bacterial cellulose. The character of wave numbers for composite membranes is on the broad band in an area of about 1091 cm^{-1}, most prominent in the infrared spectrum, according to the asymmetrical internal stretch of the vibration band SiO_2 or Al_2O_3 which is the main component of FA. While the small bands observed around 1223 cm^{-1} are for asymmetric external vibration bands of SiO_2 or Al_2O_3. The band area around 792 cm^{-1} and 600 cm^{-1} caused by symmetrical stretches of SiO_2 or Al_2O_3 and vibrations of each double ring. The small bands observed at about 600 cm^{-1} represent a bending mode for Si−O−Si. These wave numbers that have been produced are in line with the research results that have been reported (Gupta et al., 2020).

XRD characterization produces a diffractogram in Figure 4 which shows 2θ at 14.8°, 16.9°, 22.9°, 32.3°, 46.2° which are characteristic of cellulose and 2θ at 18.5°, 27.3°, 29.3°, 34.4°, 45.1°, 52.7°, 57.7° which are typical of FA (Segneanu et al., 2022). In the 2θ area at 22.9° shows an increase in intensity along with changes in the percentage of the composite made. The more FA is mixed, the higher the intensity of the XRD spectrum obtained. The difference in the intensity of crystal formation is caused by the different number of fields created in each sample, so that the amount of light reflected from the crystal field will also be different. Samples that have high intensity so that the resulting crystallinity will also be higher due to the high reflectivity of the light produced (Mubarak, 2023). Higher crystallinity in cellulose results in increased mechanical properties such as strength, stiffness, density, and hardness (Marino et al., 2015).

Figure 5 shows that the addition of fly ash to bacterial cellulose does not show any spectrum in the Raman shift other than the shift from cellulose. However, the addition of FA has an activity that causes different cellulose intensities. This is because in the composite, variations in composition, such as

changes in the ratio of fiber and matrix or the use of different types of fibers (Bokobza et al., 2017). From the Raman spectrum, there is not much change in the Raman shift, but there are several parts that show the phenomenon of composite formation, it has been revealed by researchers that it is possible to quantify the distribution and mixing of cellulose in matrix composites. The Raman shifts at 990-1020 cm^{-1} are related to C−OH out of plane bending and the C−O stretching, and region 1326 cm^{-1} show that corresponds to CH and OH wagging. For area 1460-1400 indicating to C−C stretching, and CH and OH wagging. The tangential modes are the most intensive high-energy modes of composite materials and form the so-called G-band, which is typically observed at around 1600 cm^{-1}. For this mode, the atomic displacements occur along the cicumferential direction.

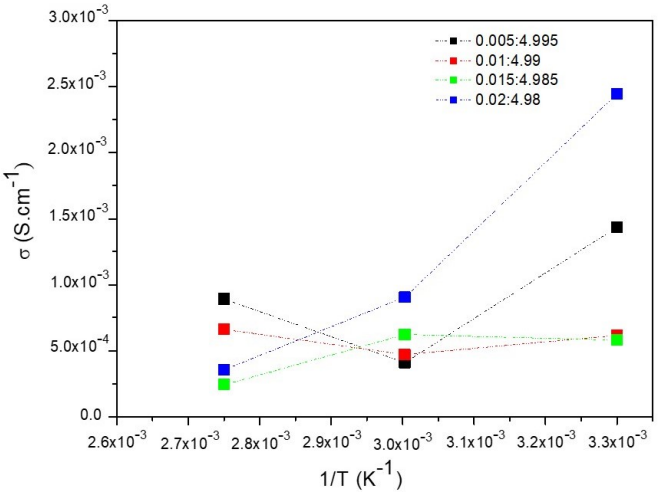

Figure 7. The Conductivity of Composite Materials at Temperatures of 30°C, 60°C and 90°C

The Raman shifts at 3100-2900 cm^{-1} are region for CH stretching vibrations. Raman spectroscopy has been utilized to study the process by which stress is transferred from the matrix to the CNs in the composites. According to reports, the cellulose band at 1095 cm^{-1} changes to lower frequencies when subjected to mechanical stress (Agarwal, 2019). Researchers have used this distinctive Raman band to examine the factors that affect stress transfer in different composite materials. Previous studies have shown that natural cellulose fibers have a well-defined Raman peak at 1095 cm^{-1}, which is associated with the C−O ring stretching. In the 1010-1095 cm^{-1} region, it generally shows weak Si−O−Si. Therefore, only a relatively narrow region between 1050 and 1150 cm^{-1} was monitored in their study (Rusli et al., 2010).

Figure 6 explains the morphology of the cellulose composite with FA obtained, a (0.005:4.995); b (0.01:4.99); c (0.015:4.985) and d (0.02:4.98). From the image, it has shown that at a magnification of 10000× it produces a morphology in the form of fibers accompanied by spheres. The fiber morphology is an image of cellulose while other forms are FA. Mass

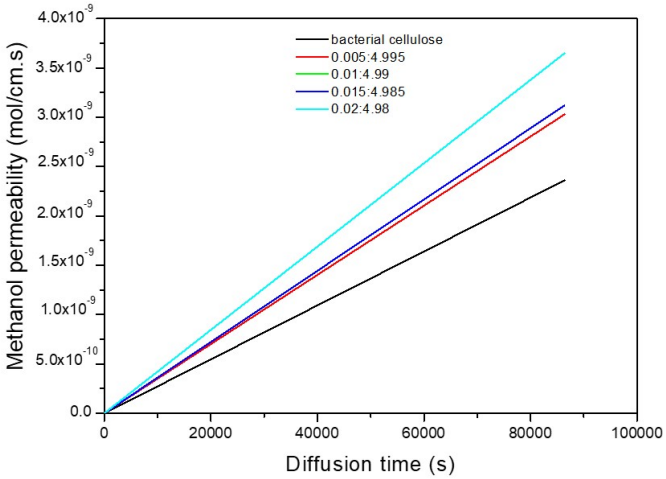

Figure 8. Methanol Permeability of Composite Materials

variations affect the number of other forms produced in the morphology of the FA cellulose composite. It can be seen in Figure 6 that with a variation of 0.02 FA, other forms are more collected in the fibers than cellulose. This also happened in previous studies in the application of nanocellulose in cementitious materials (Aofei et al., 2020).

Figure 7 shows the conductivity of the composite material. Conductivity is the ability to conduct charge in a material. Conductivity measurements were carried out using a composite material film such as a 1×1 cm membrane. The composite material was prepared by heating it at temperatures of 30°C, 60°C and 90°C using a hotplate. The heated material was then flowed with a charge through impedance. The results obtained in the conductivity process in the composite material were at a temperature of 30°C, the highest conductivity was at a variation of 0.02:4.98 which produced a conductivity of 2.45×10^{-1} S/cm. At temperature of 60°C showed the highest conductivity occurred at a variation of 0.005:4.995 which produced a conductivity of 6.22×10^{-4} S/cm and for a temperature of 90°C the conductivity obtained is 8.91×10^{-4} S/cm. All conductivities obtained from all variations and temperatures show that they are still below the order of 10^{-2} S/cm. The delivery mechanism is still influenced by water content, or the mechanism that occurs is dominated by the vehicle mechanism. The transport mechanisms rarely occur at temperatures below 100°C. This transport mechanism has been reported by Smitha et al. (2005). This result when compared with Nafion 117 of 0.086 S/cm then the value of cellulose composite with FA and cellulose is still far apart. However, the addition of FA in cellulose has an effect on the resulting conductivity.

The methanol permeability of the membrane can determine the performance of the membrane in the cell system. The membrane used in the process of determining the methanol permeability uses a membrane measuring 1×1 cm and 3 mL of methanol. After standing for 5 days with weight calculations every 24 hours, the average methanol permeability results are

obtained which has been shown in Figure 8.

From Figure 8 explain that the type of composite material films used affects the results of the methanol permeability produced. It can be seen that cellulose has the smallest permeability value of 2.37×10^{-9} mol/cm.s, while the highest permeability value occurs in the 0.02:4.98 composite material films, which is 3.66×10^{-9} mol/cm.s. For the composite material 0.01:4.99 and bacterial cellulose, the methanol permeability overlaps. The relationship between composite material films and methanol permeability shows a graph that occurs increasing along with the addition of FA to cellulose. The higher the methanol permeability produced, the lower the efficiency of the fuel cell membrane. This is due to the high surface strength and rigid nature of the film, which creates cavities in the film. This makes it more difficult for methanol to diffuse across the film. In direct methanol fuel cells, methanol crossover remains an unresolved issue, particularly for portable applications with very low current densities. Polarization losses result from fuel crossing at high methanol concentrations from the anode side to the cathode side. Similar to Sen et al. (2008) study, the methanol permeability of the composite membranes was assessed in this work using a straightforward test cell.

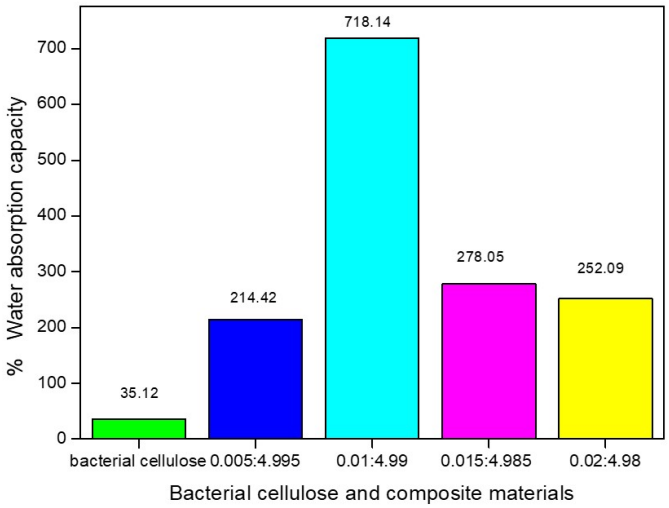

Figure 9. Water Absorption Capacity of Bacterial Cellulose and Composite Materials

Figure 9 shows the ability of the material to absorb water. The water absorption capacity of the cellulose membrane is measured by measuring the difference in membrane mass before and after immersion in water. The membrane used in this process uses a 1×1 cm membrane. The water absorption process using the membrane can be seen in Figure 9. Figure 9 shows significant and fluctuating results. When bacterial cellulose is used in the water absorption process, cellulose is able to absorb 35.12% of water. Then with the addition of FA to cellulose, the water absorption capacity increases. However, the 0.01:4.99 membrane produces the highest water absorption capacity reaching 718.14%. The addition of FA to cellulose-based materials improves the hydrophilic properties of polymer composites (Maulana et al., 2023).

4. CONCLUSIONS

Based on the research that has been done, it can be concluded that the composite between bacterial cellulose has been successfully made with fly ash (FA) with variations of 0.005:0.995; 0.01:0.99; 0.015:0.985 and 0.02:0.98. The results of the composite characterization using FTIR show the character of wave numbers for composite membranes is on the broad band in an area of about 1091 cm^{-1}, most prominent in the infrared spectrum, according to the asymmetrical internal stretch of the vibration band SiO_2 or Al_2O_3 which is the main component of FA and from the Raman shift, that show the phenomenon of composite formation, it has been revealed by researchers that it is possible to quantify the distribution and mixing of cellulose in matrix composites. From the XRD diffractogram it has been shown that there was an interaction between bacterial cellulose and FA which was accompanied by an increase in spectrum intensity. SEM morphology shows differences in the amount of FA attached to cellulose along with the addition of FA in cellulose. The conductivity value fluctuates, the methanol permeability value increases along with the addition of FA. The highest water absorption occurs in the membrane variation of 0.01:4.99.

5. ACKNOWLEDGEMENT

This work is supported by the Master of Chemistry study program, Faculty of Mathematics and Natural Sciences, University of Bengkulu with contract number from the Institute for Research and Community Service (LPPM) No: 1998/UN30.12-/HK/2024. We also thank PT. Tenaga Listrik Bengkulu, especially the TLB Public Relations Manager, Mr. Abu Bakar, who has allowed the use of FA samples.

REFERENCES

Agarwal, U. P. (2019). Analysis of Cellulose and Lignocellulose Materials by Raman Spectroscopy: A Review of the Current Status. *Molecules*, **24**(9); 1659–1675

Aofei, G., Z. Sun, N. Sathitsuksanoh, and H. Feng (2020). A Review on the Application of Nanocellulose in Cementitious Materials. *Nanomaterials*, **10**(12); 2476

Aritonang, H. F., V. S. Kamu, Ciptati, D. Onggo, and C. L. Radiman (2017). Performance of Platinum Nanoparticles/-Multiwalled Carbon Nanotubes/ Bacterial Cellulose Composite as Anode Catalyst for Proton Exchange Membrane Fuel Cells. *Bulletin of Chemical Reaction Engineering & Catalysis*, **12**(2); 287–292

Aritonang, H. F., D. Onggo, Ciptati, and C. L. Radiman (2015). Insertion of Platinum Particles in Bacterial Cellulose Membranes from $PtCl_4$and H_2PtCl_6 Precursors. *Macromolecular Symposia*, **353**(1); 55–61

Bokobza, L., M. Couzi, and J. L. Bruneel (2017). Raman

Spectroscopy of Polymer-Carbon Nanomaterial Composites. *Rubber Chemistry and Technology*, **90**(1); 37–59

Dheeresh, K. N., P. P. Abhilash, R. Singh, R. Kumar, and V. Kumar (2022). Fly Ash for Sustainable Construction: A Review of Fly Ash Concrete and Its Beneficial Use Case Studies. *Cleaner Materials*, **6**(3); 100143

Fontana, J. D., A. M. De Souza, C. K. Fontana, I. L. Torriani, J. C. Moreschi, B. J. Gallotti, S. J. De Souza, G. P. Narcisco, J. A. Bichara, and L. F. X. Farah (1990). *Acetobacter* Cellulose Pellicle as a Temporary Skin Substitute. *Applied Biochemistry and Biotechnology*, **24**; 253–264

Gopinathan, P., M. S. Santosh, V. G. Dileepkumar, T. Subramani, R. Reddy, R. E. Masto, and S. Maity (2022). Geochemical, Mineralogical and Toxicological Characteristics of Coal Fly Ash and Its Environmental Impacts. *Chemosphere*, **307**(1); 135710

Gunday, S. T., H. Tombuloglu, I. Anil, O. Alagha, and A. Bozkurt (2021). Natural Pozzolan Super-Absorbent Polymer: Synthesis, Characterization, and Its Application on Plant Growing Under Drought Condition. *International Journal of Energy and Environmental Engineering*, **12**; 751–760

Gupta, V., C. Raja, and J. Anandkumar (2020). Phenol Removal by Novel Choline Chloride Blended Cellulose Acetate-Fly Ash Composite Membrane. *Periodica Polytechnica Chemical Engineering*, **64**(1); 116–123

Henrik, B., G. Helenius, A. Bodin, U. Nannmark, B. R. Johansson, B. Risberg, and P. Gatenholm (2006). Mechanical Properties of Bacterial Cellulose and Interactions with Smooth Muscle Cells. *Biomaterials*, **27**(9); 2141–2149

Iguchi, M., S. Yamanaka, and A. Budhiono (2000). Bacterial Cellulose-A Masterpiece of Nature's Arts. *Journal of Materials Science*, **35**(2); 261–270

Joel, S. (2020). Compressive Strength of Concrete Using Fly Ash and Rice Husk Ash: A Review. *Civil Engineering Journal*, **6**(7); 1400–1410

Kim, S. H., C. M. Lee, and K. Kafle (2013). Characterization of Crystalline Cellulose in Biomass: Basic Principles, Applications, and Limitations of XRD, NMR, IR, Raman, and SFG. *Korean Journal of Chemical Engineering*, **30**; 2127–2141

Kumar, P. N., A. Rajadurai, and T. Muthuramalingam (2018). Multi-Response Optimization on Mechanical Properties of Silica Fly Ash Filled Polyester Composites Using Taguchi-Grey Relational Analysis. *Silicon*, **10**(4); 1723–1729

Marino, M., L. L. D. Silva, N. Duran, and L. Tasic (2015). Enhanced Materials from Nature: Nanocellulose from Citrus Waste. *Molecules*, **20**(4); 5908–5923

Maulana, F., M. P. Aulia, and S. Aprilia (2023). Fly Ash/-Coconut Fiber Reinforced Polymer Composites: Effect on Physical Properties (Density, Water Absorption, and Thickness Swelling). *Materials Today: Proceedings*, **87**(2); 180–186

Moon, H. K., J. E. Kim, J. Go, E. K. Koh, S. H. Song, H. J. Son, H. S. Kim, Y. H. Yun, Y. J. Jung, and D. Y. Hwang (2015). Bacterial Cellulose Membrane Produced by *Acetobacter* sp. A10 for Burn Wound Dressing Applications. *Carbohydrate Polymers*, **122**(20); 387–398

Moon, S. H., J. M. Park, H. Y. Chun, and S. J. Kim (2006). Comparisons of Physical Properties of Bacterial Celluloses Produced in Different Culture Conditions Using Saccharified Food Wastes. *Biotechnology and Bioprocess Engineering*, **11**(1); 26–31

Mubarak, A. (2023). Qualitative Analyses of Thin Film-Based Materials Validating New Structures of Atoms. *Materials Today Communications*, **36**; 106552

Muhammad, M. A., M. C. I. M. Amin, and C. Martin (2014). A Review of Bacterial Cellulose-Based Drug Delivery Systems: Their Biochemistry, Current Approaches and Future Prospects. *Journal of Pharmacy and Pharmacology*, **66**(8); 1047–1061

Mutiara, T., H. Sulistyo, M. Fahrurrozi, and M. Hidayat (2022). Facile Route of Synthesis of Silver Nanoparticles Templated Bacterial Cellulose, Characterization, and Its Antibacterial Application. *Green Processing and Synthesis*, **11**(2); 361–372

Nishi, Y., M. Uryu, S. Yamanaka, K. Watanabe, N. Kitamura, M. Iguchi, and S. Mitsuhashi (1990). The Structure and Mechanical Properties of Sheets Prepared from Bacterial Cellulose. *Journal of Materials Science*, **25**(6); 2997–3001

Norhaiza, G., K. Muthusamy, and S. W. Ahmad (2019). Utilization of Fly Ash in Construction. In *IOP Conference Series: Materials Science and Engineering*, volume 601. page 012023

Prayoga, M. B. R. and R. A. Afla (2023). Utilization of Fly Ash and Bottom Ash Waste: A Study at PLTU Tanjung Jati B, Jepara, Indonesia. *Asian Journal of Toxicology, Environmental, and Occupational Health*, **1**(1); 9–19

Radiman, C. L. and A. Rifathin (2013). Preparation of Phosphorylated Nata-de-Coco for Polymer Electrolyte Membrane Applications. *Journal of Applied Polymer Science*, **130**(1); 399–405

Radiman, C. L. and G. Yuliani (2008). Coconut Water as a Potential Resource for Cellulose Acetate Membrane Preparation. *Polymer International*, **57**(3); 502–508

Rahmawati, S., C. L. Radiman, and M. A. Martoprawiro (2018). Density Functional Theory (DFT) and Natural Bond Orbital (NBO) Analysis of Intermolecular Hydrogen Bond Interaction in Phosphorylated Nata de Coco-Water. *Indonesian Journal of Chemistry*, **18**(1); 173–178

Refaat, A., H. Elhaes, and M. A. Ibrahim (2023). Effect of Alkali Metals on Physical and Spectroscopic Properties of Cellulose. *Scientific Reports*, **13**; 21649

Rusli, R., K. Shanmuganathan, S. J. Rowan, C. Weder, and S. J. Eichhorn (2010). Stress-Transfer in Anisotropic and Environmentally Adaptive Cellulose Whisker Nanocomposites. *Biomacromolecules*, **11**(3); 762–768

Satapathy, S., A. Nag, and G. Nando (2012). Effect of Electron Beam Irradiation on the Mechanical, Thermal, and Dynamic Mechanical Properties of Fly Ash and Nanostructured Fly Ash Waste Polyethylene Hybrid Composites. *Polymer Composites*, **33**(1); 109–119

Segneanu, A. E., C. N. Marin, G. Vlase, C. Cepan, M. Mihailescu, C. Muntean, and I. Grozescu (2022). Highly Ef-

ficient Engineered Waste Eggshell-Fly Ash for Cadmium Removal from Aqueous Solution. *Scientific Reports*, **12**(1); 9676–96108

Seham, S. A. and N. H. Marei (2021). Fly Ash Properties, Characterization, and Applications: A Review. *Journal of King Saud University-Science*, **33**(6); 101536

Sen, U., S. U. Celik, A. Ata, and A. Bozkurt (2008). Anhydrous Proton Conducting Membranes for PEM Fuel Cells Based on Nafion/Azole Composites. *International Journal of Hydrogen Energy*, **33**(11); 2808–2815

Shao, W., H. Liu, S. Wang, J. Wu, M. Huang, H. Min, and X. Liu (2016). Controlled Release and Antibacterial Activity of Tetracycline Hydrochloride-Loaded Bacterial Cellulose Composite Membranes. *Carbohydrate Polymers*, **145**; 114–120

Shibazaki, H., S. Kuga, F. Onabe, and M. Usuda (1993). *Bacterial Cellulose* Membrane as Separation Medium. *Journal of Applied Polymer Science*, **50**(6); 965–969

Siregar, S. M., S. Humaidi, N. Bukit, and E. Frida (2024). Palm Oil Fuel Ash and Fly Ash for a Partial Replacement of Cement in High-Quality, Environmentally Friendly Mortar as a Solution to Industrial Waste. *Science and Technology Indonesia*, **9**(1); 59–68

Smitha, B., S. Sridhar, and A. A. Khan (2005). Chitosan-Sodium Alginate Polyion Complexes as Fuel Cell Membranes. *European Polymer Journal*, **41**(8); 1859–1866

Sulaeva, I., U. Henniges, T. Rosenau, and A. Potthast (2015). Bacterial Cellulose as a Material for Wound Treatment: Properties and Modifications. *Biotechnology Advances*, **33**(8); 1547–1571

Tahara, N., M. Tabuchi, K. Watanabe, H. Yano, Y. Morinaga, and F. Yoshinaga (1997). Degree of Polymerization of Cellulose From *Acetobacter xylinum* BPR2001 Decreased by Cellulase Produced by the Strain. *Bioscience, Biotechnology and Biochemistry*, **61**(11); 1862–1865

Thomas, S. (2008). A Review of the Physical, Biological and Clinical Properties of a Bacterial Cellulose Wound Dressing. *Journal of Wound Care*, **17**(8); 349–352

Visa, M. (2016). Synthesis and Characterization of New Zeolite Materials Obtained From Fly Ash for Heavy Metals Removal in Advanced Wastewater Treatment. *Powder Technology*, **294**; 338–347

